

Diversity in a Simple Co-crystal: Racemic and Kryptoracemic Behaviour

U. B. Rao Khandavilli, Matteo Lusi, Balakrishna R. Bhogala, Anita R. Maguire, M. Stein,
Simon E. Lawrence*

simon.lawrence@ucc.ie

Supporting Information

	Page
IR spectra for Forms I and III	S2
Raman spectra for Forms I and III	S2
DSC data for Forms I and III	S3
Summary crystallographic data	S3
PXRD data for Forms I and III	S4
Selected torsion angles for the amide molecules in Forms I, II and III	S5
Polymorph screen	S6
Microscopy images of Forms I and III	S6
Precession photos for Forms I and II	S7
Details of periodic DFT calculations	S9
Slurry Experiments	S10

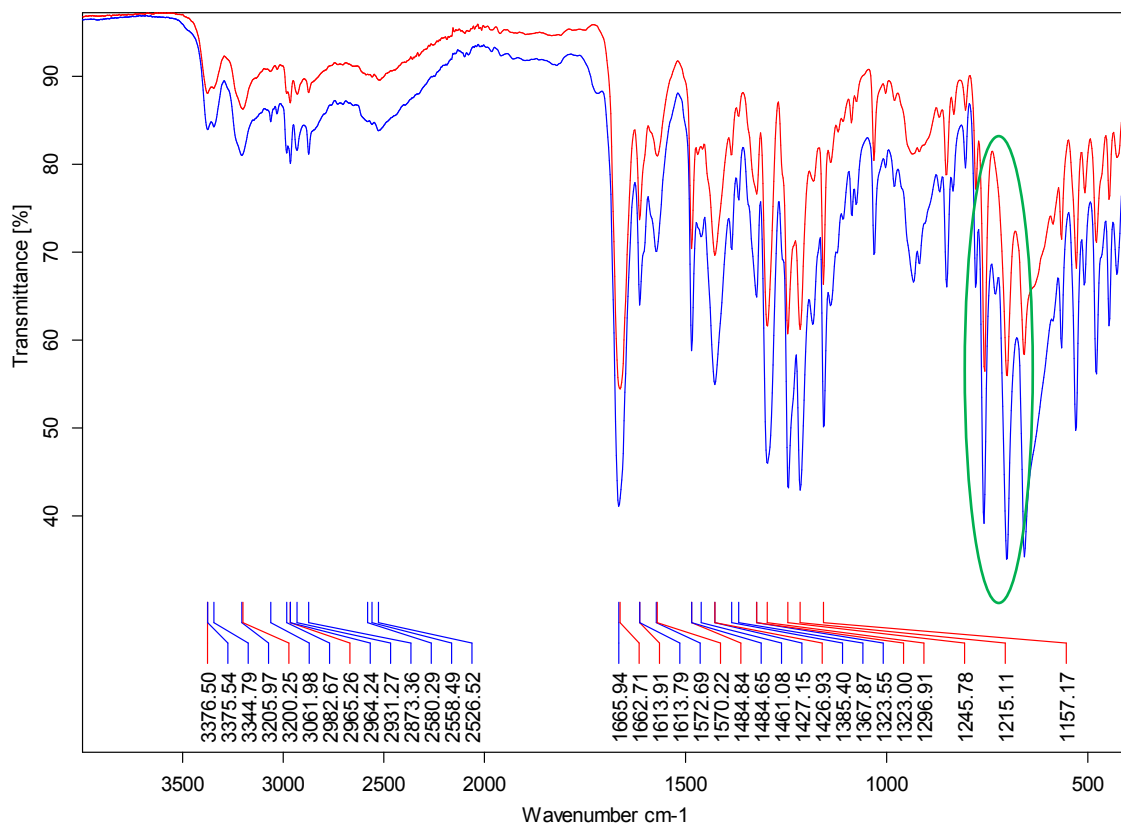


Figure 1. IR spectra for Forms I (blue) and Form III (red): the green circle highlights an extra peak in Form I

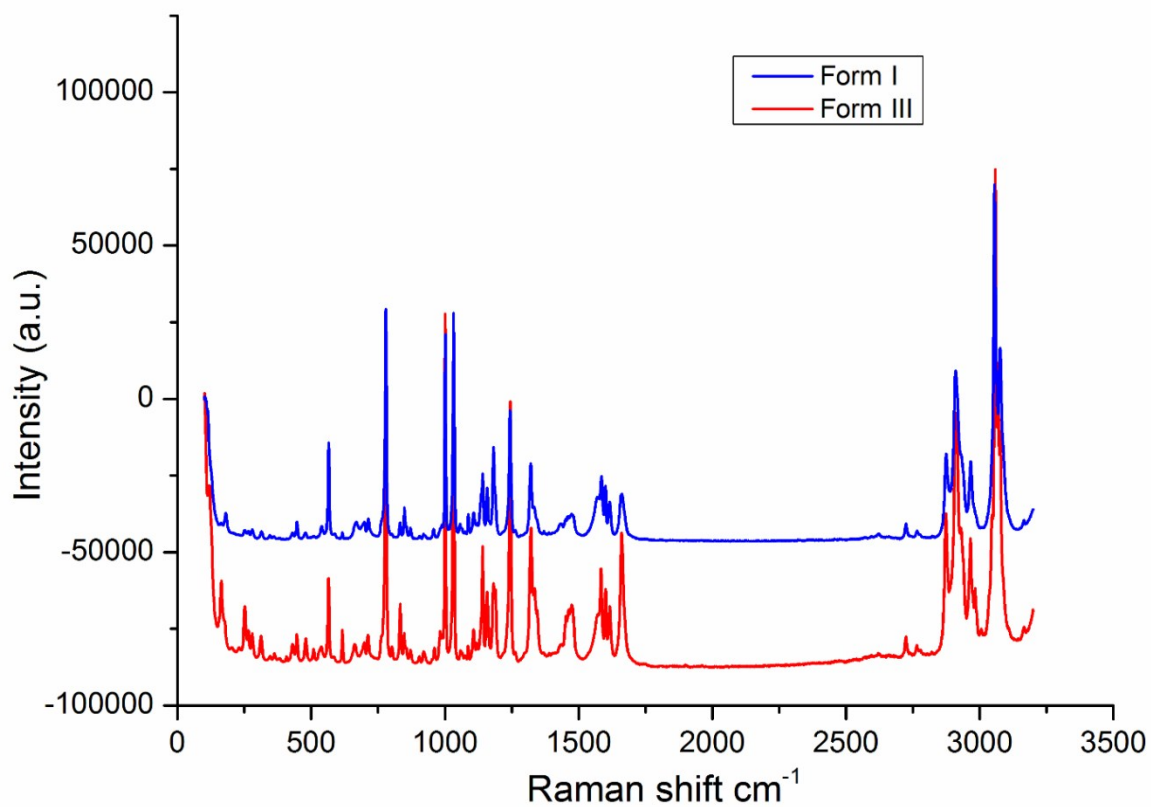


Figure 2. Raman spectra for Forms I (blue) and Form III (red)

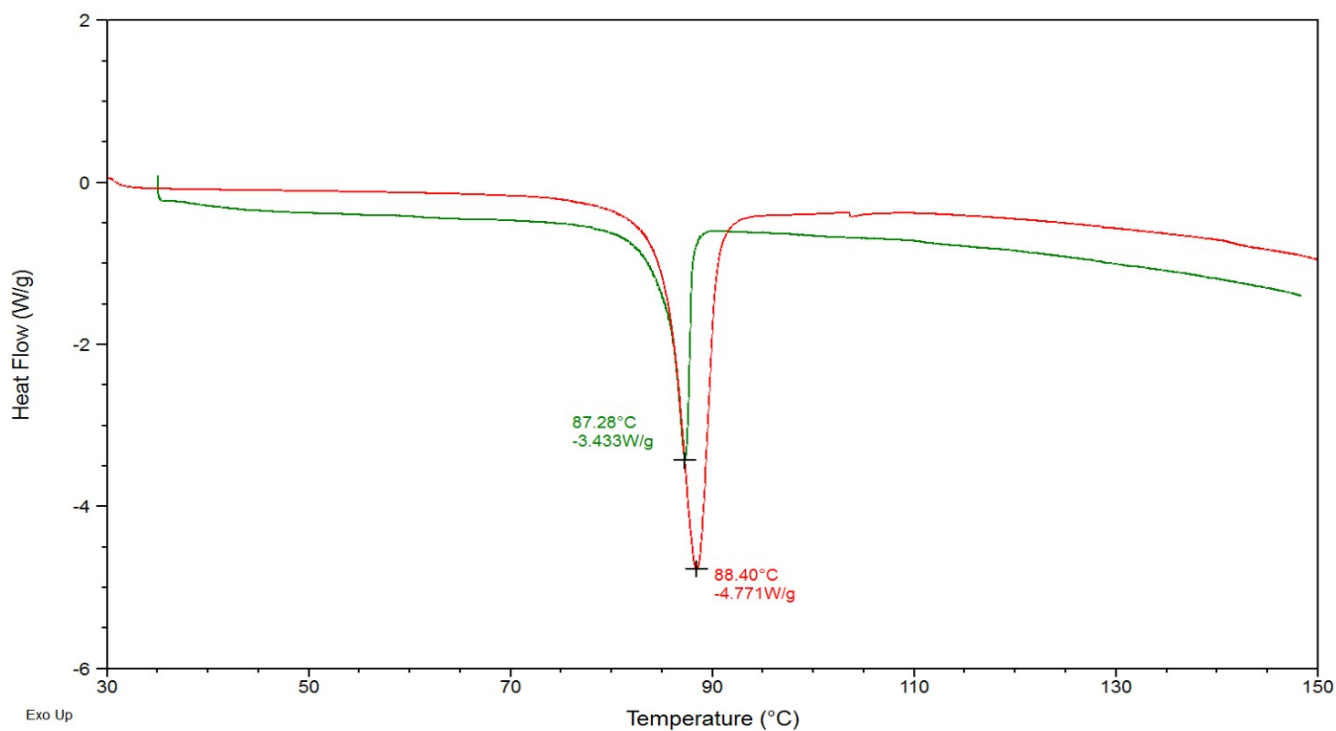


Figure 3. DSC data for Forms I (green) and Form III (red)

Table 1. Summary crystallographic data

	Form I	Form II	Form III
Crystal System	orthorhombic	monoclinic	monoclinic
Space Group, <i>Z</i>	<i>P2₁2₁2₁</i> , 4	<i>P2₁</i> , 2	<i>P2₁/c</i> , 4
<i>a</i> , Å	10.0924(6)	9.882(4)	10.0661 (14)
<i>b</i> , Å	16.2467(12)	20.953(8)	21.081(3)
<i>c</i> , Å	21.2038(15)	16.215(6)	16.584(2)
α , °	90	90	90
β , °	90	93.913(11)	100.060(4)
γ , °	90	90	90
<i>V</i> , Å ³	3476.8(4)	3350.0(2)	3465.1(8)
<i>D_c</i> gcm ⁻³	1.174	1.251	1.209
<i>T</i> , K	300	100	300

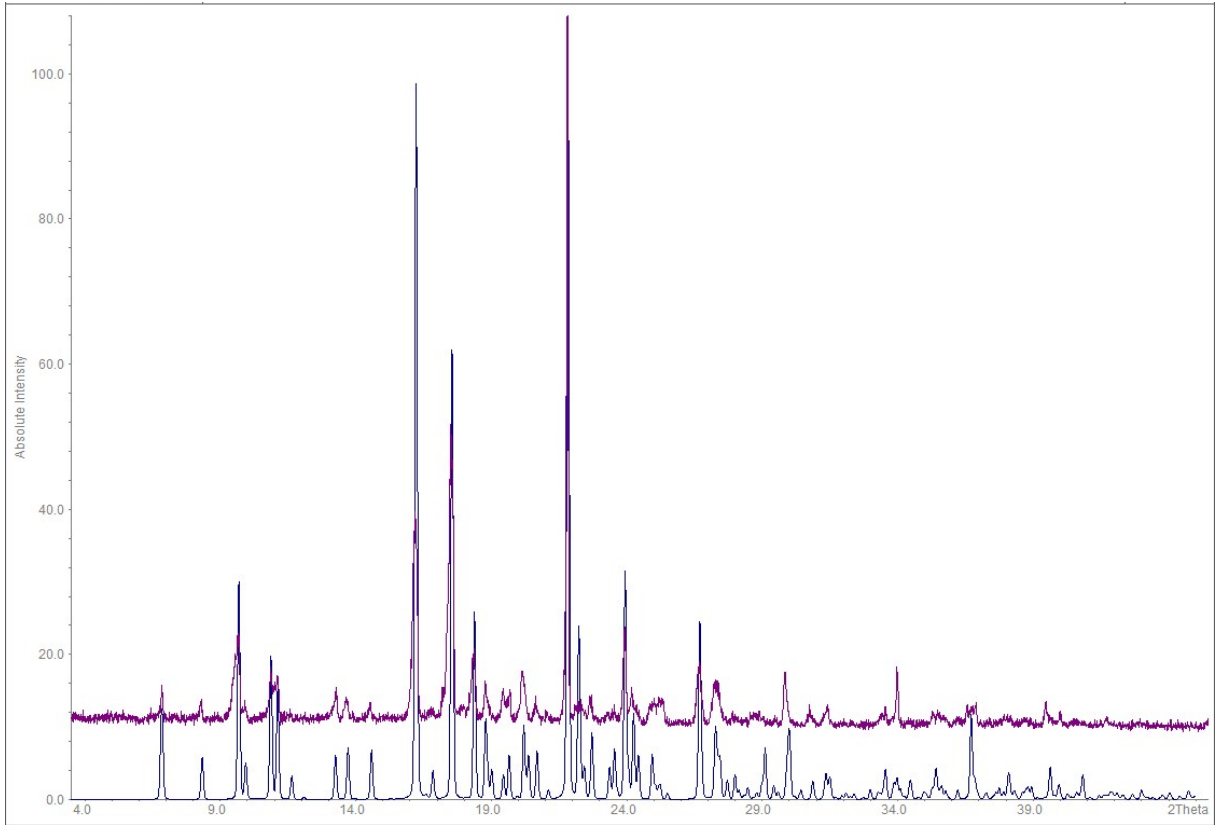


Figure 4. PXR D data for Form I: experimental (purple) and theoretical (blue)

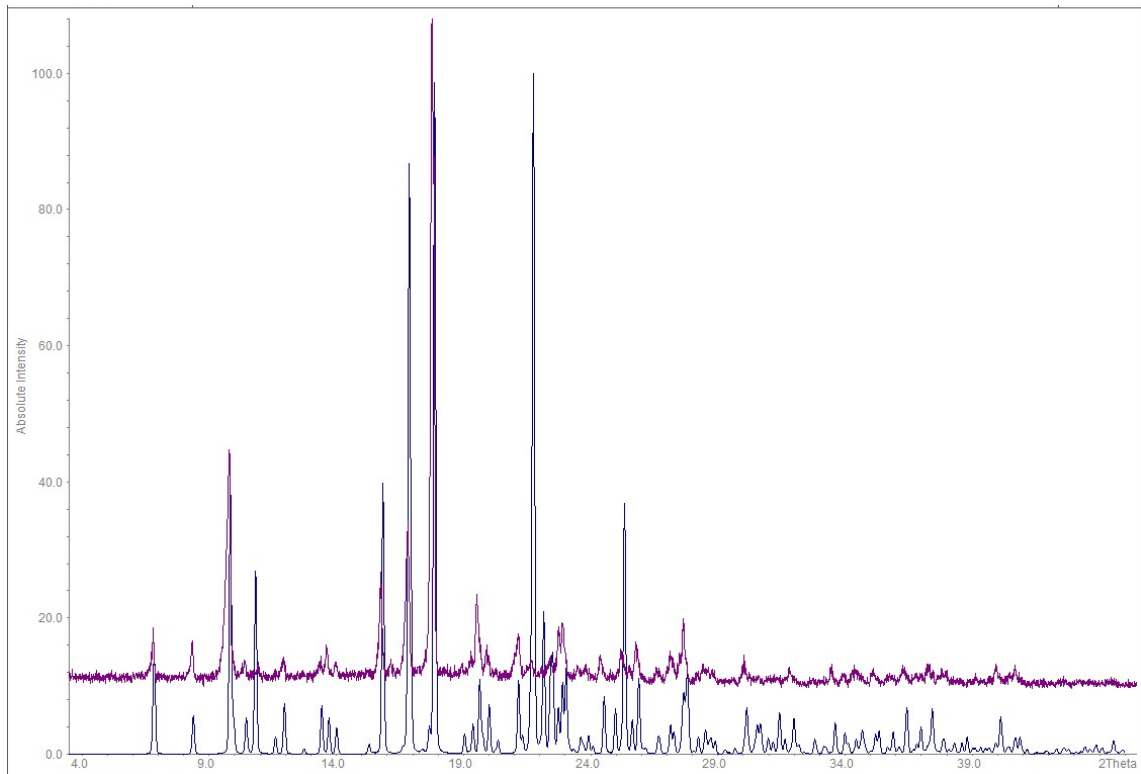


Figure 5. PXR D data for Form III: experimental (purple) and theoretical (blue)

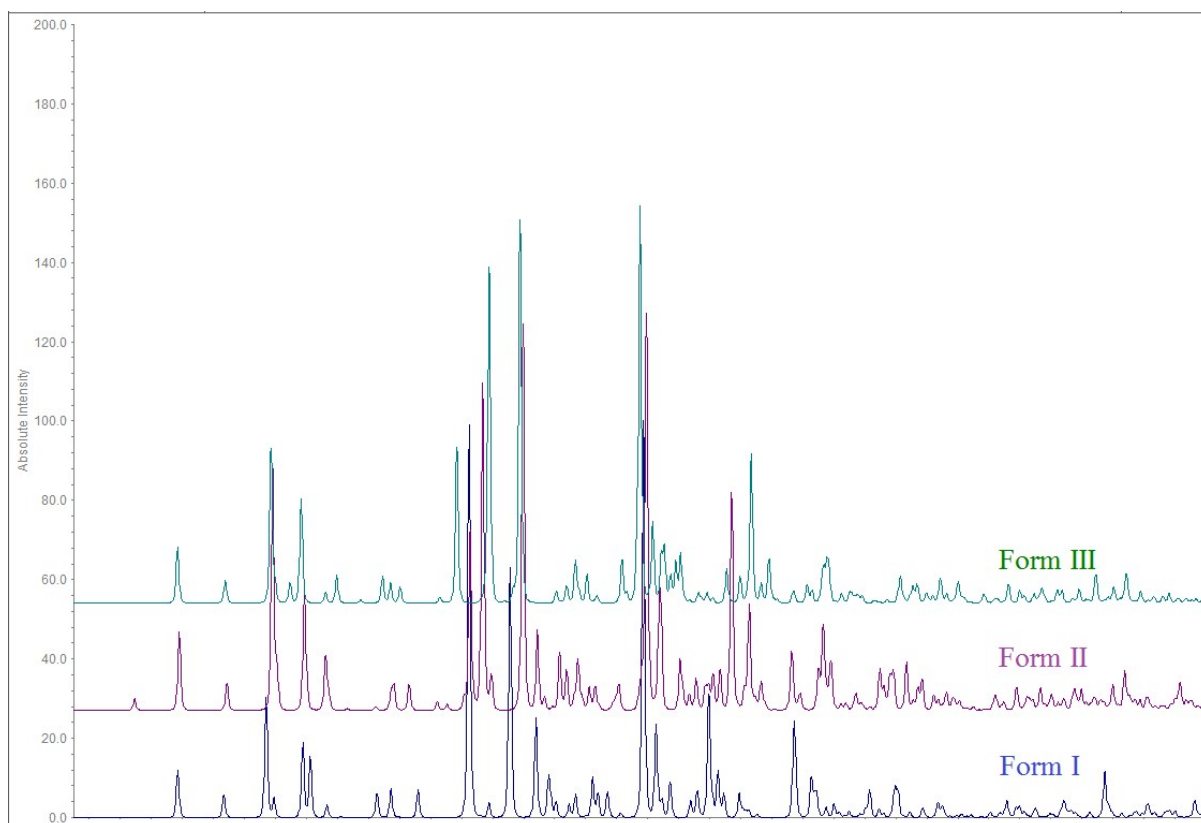
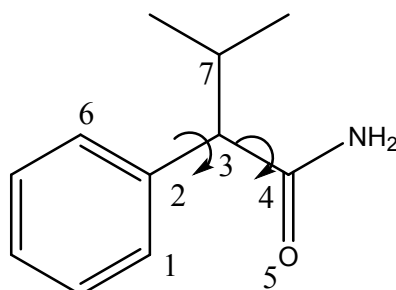


Figure 6. Theoretical PXRD data for Forms I, II & III.

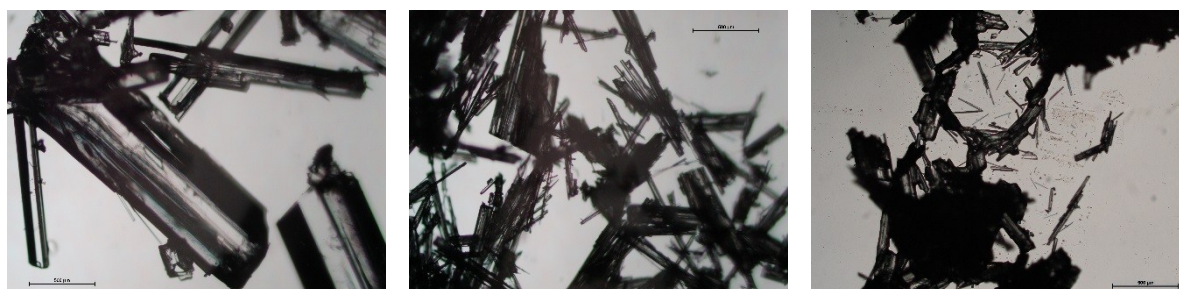
Table 2. Selected torsion angles for the amide molecules in Forms I, II and III



	Z'	Molecule	τ_1 C1-C2-C3-C4	τ_2 C6-C2-C3-C7	τ_3 C2-C3-C4-O5	τ_4 C2-C3-C4-O5
Form I	2	R1	51.01	101.94	-88.20	-142.82
		S2	-52.13	-105.18	82.68	138.41
Form II	4	R1	55.51	106.93	-91.21	-143.77
		S2	-44.27	-92.75	96.55	150.43
		R3	51.24	102.79	-76.49	-130.71
		S4	-55.72	-111.14	75.24	132.52
Form III	2	R1	53.66	106.63	-87.40	-143.36
		S2	-50.46	-102.04	92.61	148.74

Table 3. Polymorph screen

Solvent(s)	Temperature: ~ 18 °C	Temperature: ~ 1 °C
Acetone	Form I	Form I
Acetonitrile	Form I	Form I
Diethyl ether	Form I	Form I
Methanol	Form I	Form I
Tetrahydrofuran	Form I	Form I
Toluene + Methanol	Form I	Form I
Ethanol	Form I	Form I + Form III
Ethyl acetate	Form I	Form I + Form III
Hexane	Form I	Form I + Form III
Chloroform + Methanol	Form I	Form I + Form-III
Hexane + Dichloromethane	Form I	Form I + Form III
Hexane + Methanol	Form I	Form I + Form III
Dichloromethane	Form I	Form III

**Figure 7.** Microscopic images of Form I, Form III and concomitant crystals respectively

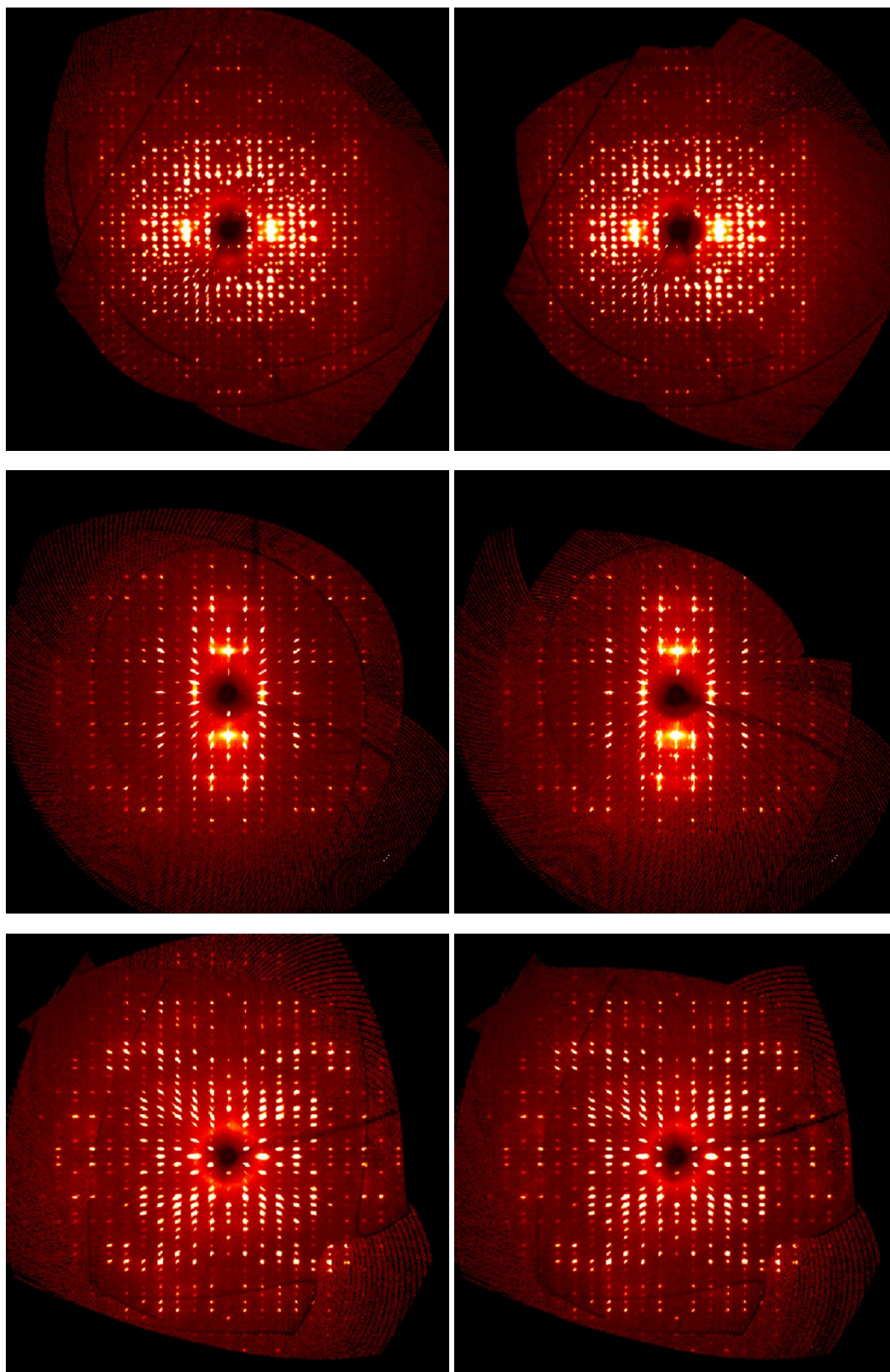


Figure 8. Side to side comparison of the precession images for the cocystal collected at 250 K for the 0kl (top), h0l (centre) and hk0 (bottom) planes. Left: before cooling to 100 K, Right: after cooling.

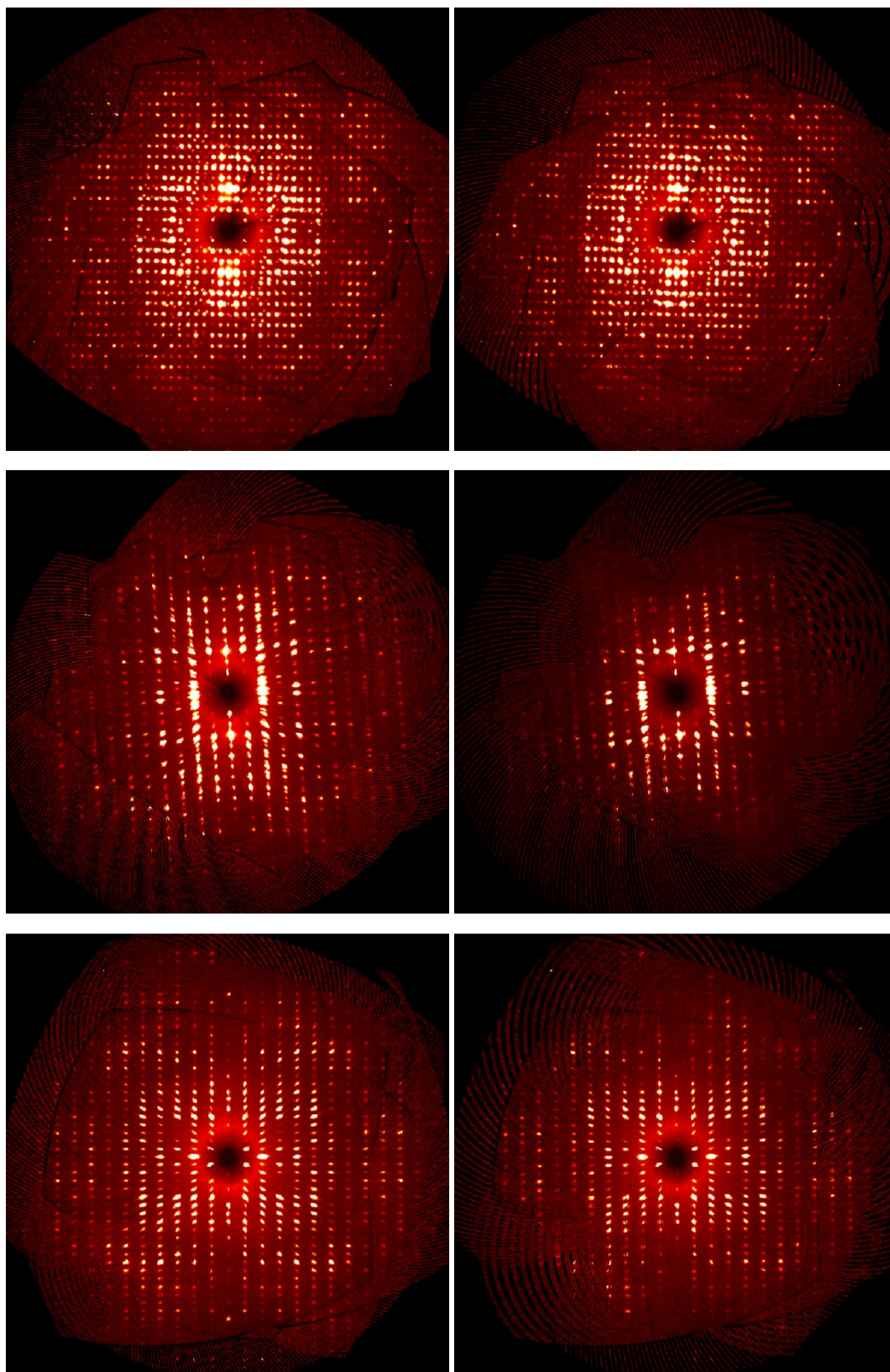


Figure 9. Side to side comparison of the precession images for the cocrystal at 150 K (left) and 100 K (right) for the 0kl (top), h0l (centre) and hk0 (bottom) planes.

Details of periodic DFT calculations

Periodic electronic structure methods for organic crystals based on density functional theory with an essential correction to account for dispersion interaction can generate a reliable energy ranking of different possible crystal structures. Here, the periodic DFT code BAND 2014.¹ was used with Slater atomic orbitals and a TZP basis set for all atoms with the 1s orbitals frozen for oxygen, nitrogen and carbon atoms². γ -point calculations were performed (k-space = 1). Initially, only the positions of the hydrogen atoms were optimized and later all atomic positions were unconstrained. The number of basis functions amounted to 4136 for each calculation.

The BP86³ and the revPBE⁴ exchange-correlation functionals both with Grimme's correction for van-der-Waals interactions⁵ and Becke-Johnson damping were used. The PBE functional was shown to yield superior crystal energy landscapes for organic and pharmaceutical non-chiral and chiral structures.

Default convergence criteria of SCF energies, energy conversion and structural optimizations were used.

¹ a) BAND2014, SCM, Theoretical Chemistry, Vrije Universiteit, Amsterdam, The Netherlands, <http://www.scm.com>. b) G. te Velde and E.J. Baerends, *Physical Review B* **44**, 7888 (1991).

² E. van Lenthe and E.J. Baerends, *Journal of Computational Chemistry* **24**, 1142 (2003).

³a) A.D. Becke, *Physical Review A* **38**, 3098 (1988). b) J.P. Perdew and Y. Wang, *Physical Review B* **33**, 8800 (1986).

⁴a) J.P. Perdew, K. Burke and M. Ernzerhof, *Physical Review Letters* **77**, 3865 (1996). b) Y. Zhang and W. Yang, *Physical Review Letters* **80**, 890 (1998).

⁵S. Grimme, S. Ehrlich, and L. Goerigk, *Journal of Computational Chemistry* **32**, 1457 (2011).

Relative total lattice energies in kcal/mol	Form I	Form II	Form III
	Kryptoracemate, P ₂₁₂₁₂₁	Kryptoracemate, P ₂₁	Mono-racemic, P _{21/c}
BP86-D3(BJ)/TZP//single crystal structure	+369.7	0.0	-67.5
BP86-D3(BJ)/TZP//opt Hs	+34.7	0.0	+2.0
revPBE-D3(BJ)/TZP//BP86-D3(BJ) opt Hs	+31.3	+11.7	0.0
revPBE-D3(BJ)/TZP//revPBE-D3(BJ)/TZP optHs	+31.0	+8.3	0.0

Slurry Experiments

Starting Composition	Product
Form I (pure)	Form I
Form I (80%) + Form III (20%)	Form III
Form I (20%) + Form III (80%)	Form III
Form III (pure)	Form III

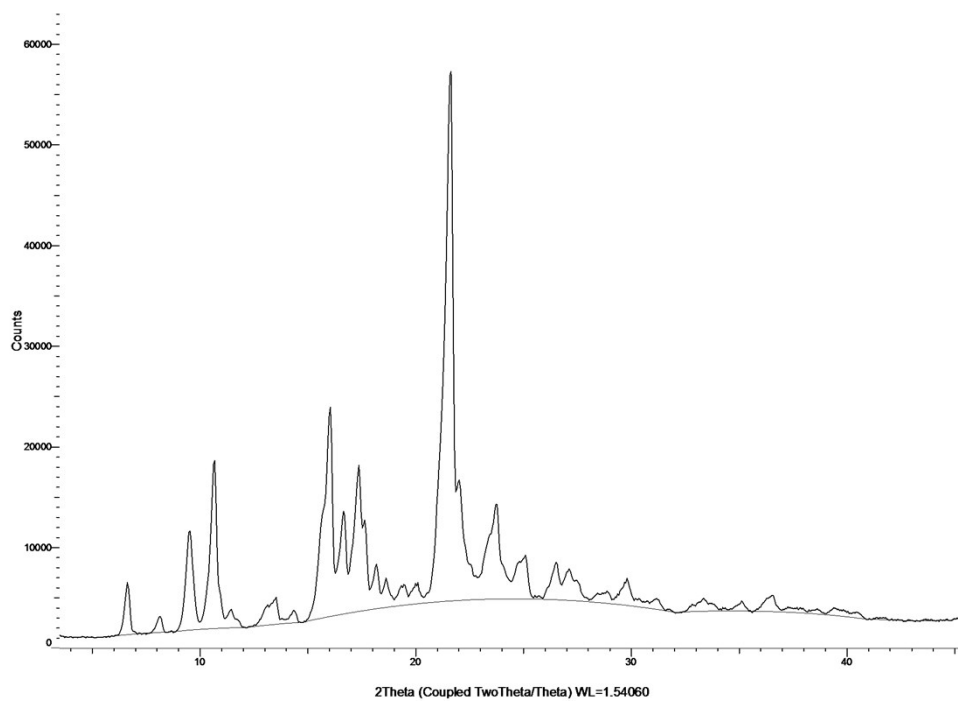


Figure 10. Form I obtained from pure Form I starting composition.

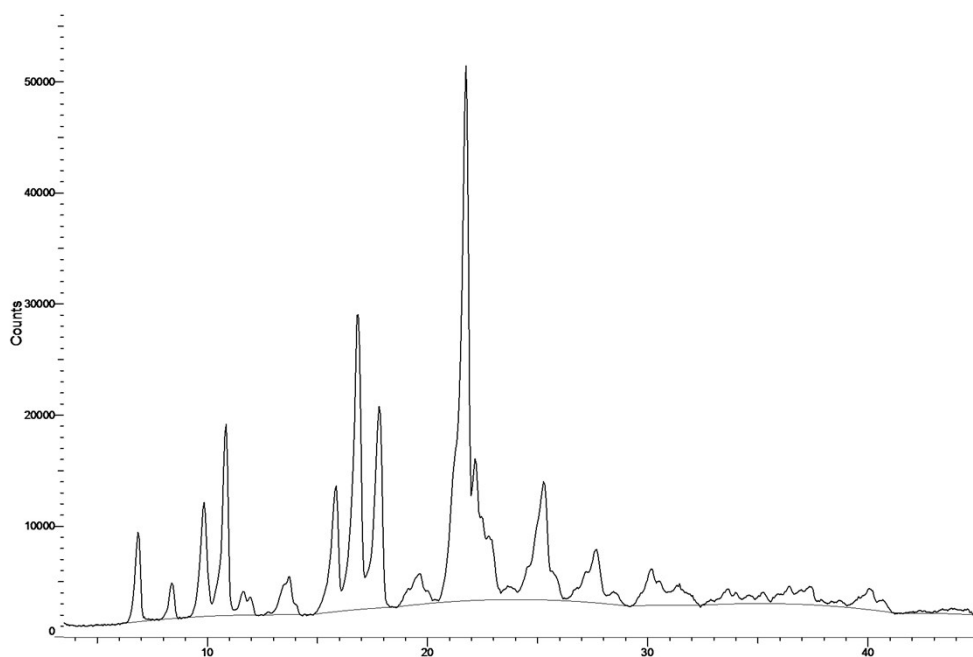


Figure 11. Form III obtained from Form I : Form III 80% : 20% starting composition.

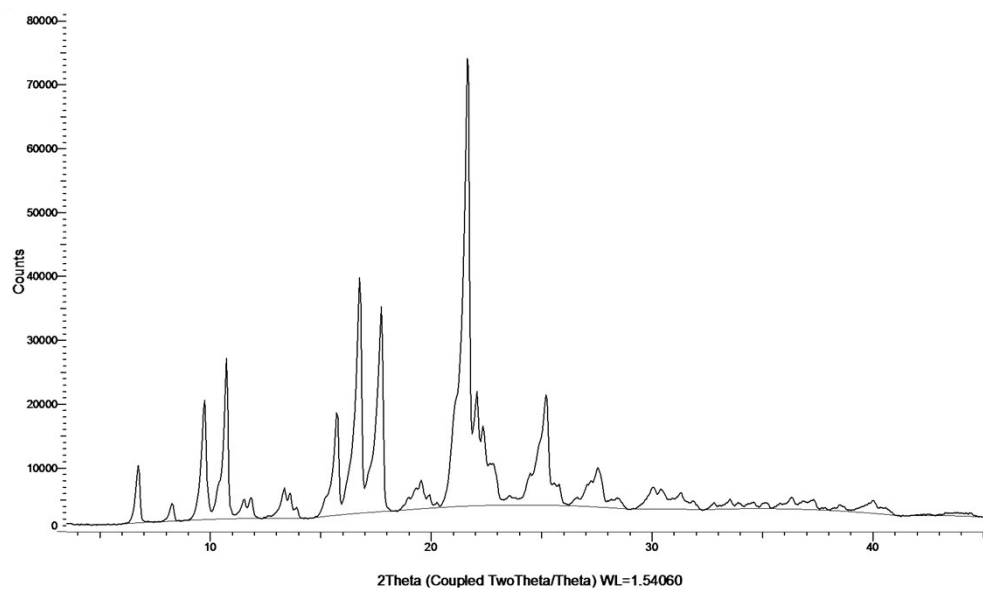


Figure 12. Form III obtained from Form I : Form III 20% : 80% starting composition

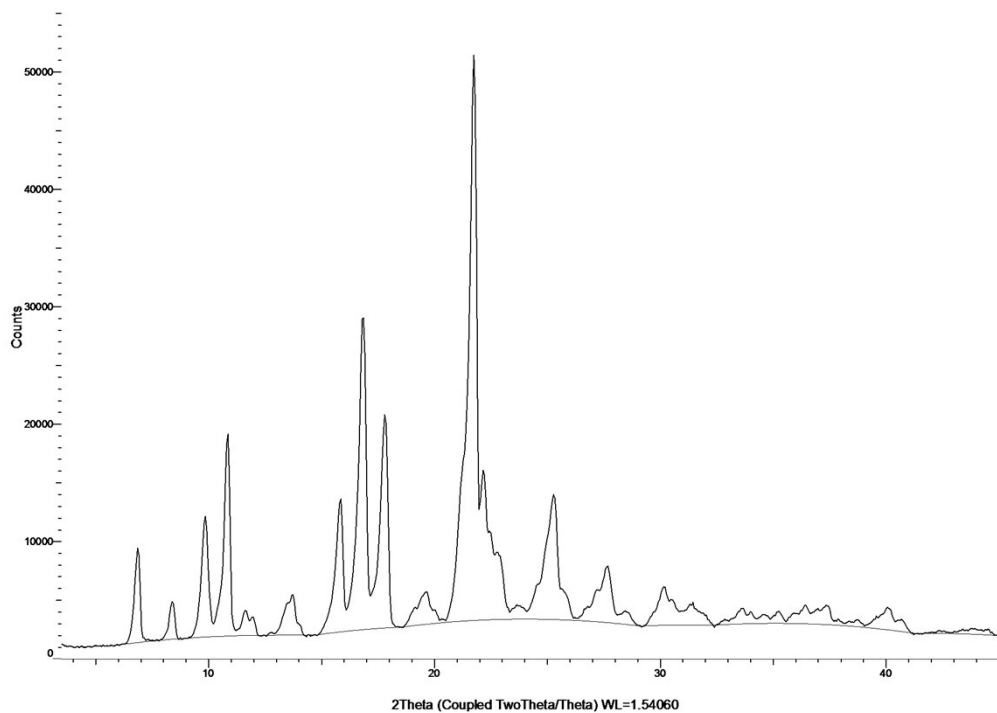


Figure 13. Form III obtained from pure Form III starting composition.